NOTES AND CORRESPONDENCE

Aspects of a Tornadic Left-Moving Thunderstorm of 25 May 1999

JOHN F. DOSTALEK

Cooperative Institute for Research in the Atmosphere, Colorado State University, Fort Collins, Colorado

JOHN F. WEAVER

NOAA/NESDIS/RAMM Team, Colorado State University, Fort Collins, Colorado

G. LOREN PHILLIPS[*]

National Weather Service Forecast Office, Lubbock, Texas

13 February 2003 and 24 November 2003

ABSTRACT

A severe left-moving thunderstorm occurred on 25 May 1999 between the cities of Lubbock and Amarillo, Texas. Over its 3.5-h lifetime, the storm was responsible for flash flooding, reports of hail of up to 7 cm in diameter, and two weak tornadoes. Satellite imagery reveals that it was traveling along the northward-moving outflow boundary of the storm from which it formed. The left mover displayed anticyclonic rotation, as was seen in storm-relative radial velocity imagery from the Weather Surveillance Radar-1988 Doppler (WSR-88D) located at Lubbock. The tornadoes developed west of Canyon, Texas, near the intersection of the left mover and a southward-moving boundary. The occurrence of tornadoes with a left mover is a particularly noteworthy event; to the authors' knowledge, only four other tornadic left movers have been reported in the meteorological literature.

1. Introduction

Because of their inherent dangers to life and property, severe thunderstorms have rightly received widespread attention in the meteorological literature. One class of severe thunderstorm that produces some of the most damaging weather is the supercell. These storms contain a cyclonically (anticyclonically) rotating updraft and have a propagational component to the right (left) of the vertical wind shear vector. For vertical wind profiles typical of severe weather environments in the United States, a cyclonically rotating updraft (mesocyclone) also moves to the right of the mean wind and an anticyclonically rotating updraft (mesoanticyclone) moves to the left of the mean wind. Although Davies-Jones (1985) reports that right-moving mesocyclones are more

prevalent than left-moving mesoanticyclones, left-moving supercells do exist and can produce severe weather (Hammond 1967; Nielsen-Gammon and Read 1995; Grasso and Hilgendorf 2001; Monteverdi et al. 2001). This note adds to the existing literature on severe left-moving thunderstorms by examining an event that occurred on 25 May 1999 in northwest Texas, between the cities of Lubbock and Amarillo. This particular storm is noteworthy because two tornadoes were reported with the storm. Few tornadic left movers have been documented in the literature.

The paper is divided into three subsequent sections. Section 2 provides an overview of the convective environment of 25 May 1999. The characteristics of the left mover are discussed in section 3. A summary of the event is given in section 4.

* Current affiliation: Atmospheric Science Group, Texas Tech University, Lubbock, Texas.

Corresponding author address: John F. Dostalek, Research Associate, CIRA, Colorado State University, 1375 Campus Delivery, Fort Collins, CO 80523-1375.
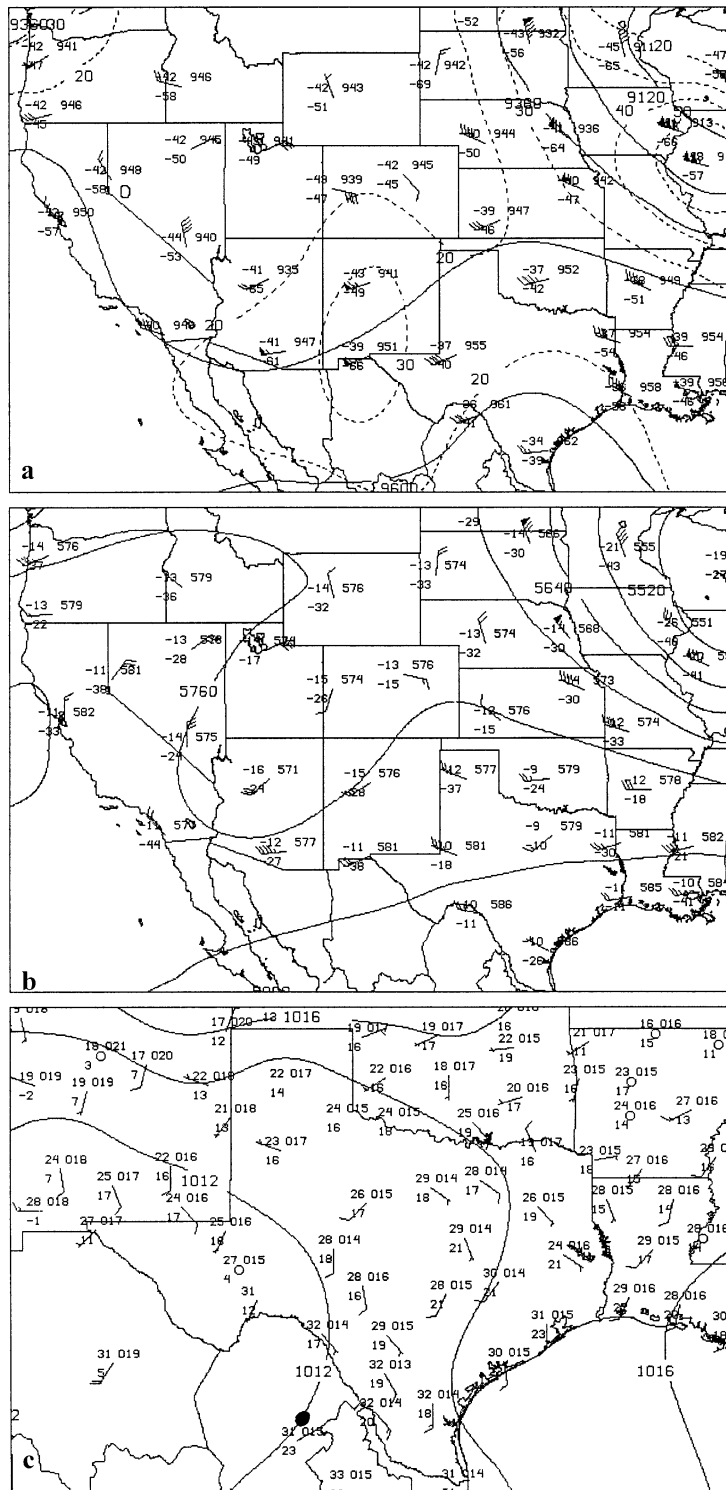E-mail: dostalek@cira.colostate.edu

2. Initial thunderstorm development

a. Synoptic-scale overview

A 300-hPa trough was positioned over the southwestern United States at 1200 UTC 25 May 1999. Winds at the southern and eastern side of the trough were from

FIG. 1. At 1200 UTC 25 May 1999, (a) 300-hPa heights (m; contour interval is 120 m), isotachs (m s^{-1}; contour interval 10 is m s^{-1} with contours below 20 m s^{-1} omitted), and station plots and (b) 500-hPa heights (m; contour interval is 60 m) and station plots. (c) At 1800 UTC 25 May 1999, mean sea level pressure (hPa; contour interval is 2 hPa) and surface station plots. The 300- and 500-hPa station plots show (counterclockwise from upper right) height (dam), temperature (°C), and dewpoint temperature (°C). Surface station plots show (counterclockwise from upper right) mean sea level pressure (tenths of hectopascals with leading 10 dropped), temperature (°C), and dewpoint temperature (°C). For (a)–(c), a half wind barb is equal to 2.5 m s^{-1}, a full wind barb is equal to 5 m s^{-1}, and a pennant is equal to 25 m s^{-1}.
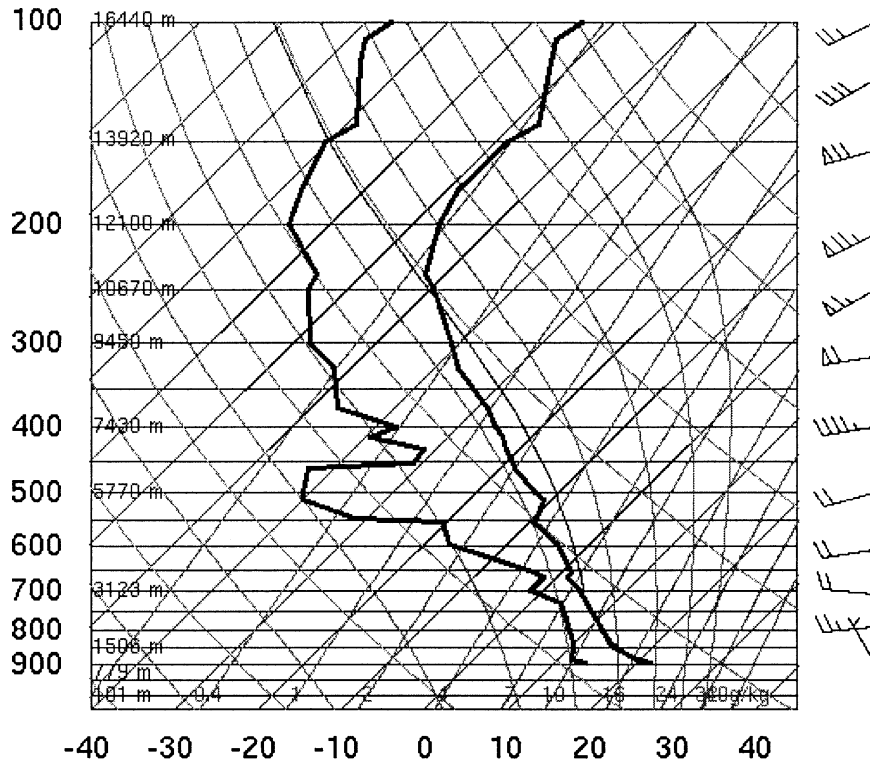
FIG. 2. The 1800 UTC 25 May 1999 sounding from Amarillo, TX. A half wind barb is equal to 2.5 m s^{-1}, a full wind barb is equal to 5 m s^{-1}, and a pennant is equal to 25 m s^{-1}. Plot is courtesy of the University of Wyoming.

the west-southwest at 20 m s^{-1}, with an embedded area of winds exceeding 30 m s^{-1} over New Mexico (Fig. 1a). At 500 hPa, a positively tilted trough extended from southeastern California to southeastern Wyoming. A ridge axis located over west Texas was situated downstream of the trough and provided northwest winds of around 15 m s^{-1} to the area (Fig. 1b). At 1800 UTC, a broad surface trough covered much of Texas and was accompanied by south-southeasterly winds in the eastern two-thirds of the state (Fig. 1c). In the western third of the state, surface winds were weaker and were from the west or southwest. Temperatures decreased from south to north, with values around 30°C in south Texas to below 20°C in parts of New Mexico, Oklahoma, and Arkansas (Fig. 1c).

b. The onset of deep moist convection

Moisture, instability, and a lifting mechanism are identified by Johns and Doswell (1992) as necessary for the realization of deep moist convection. The dewpoint temperatures in northwest Texas at 1800 UTC 25 May 1999 were around 15°C (Fig. 1c). The low-level moisture had a depth of about 250 hPa, extending from the surface to 650 hPa, as is seen in the 1800 UTC sounding from Amarillo (Fig. 2).

Convective available potential energy (CAPE) was utilized as a measure of the instability of the atmosphere.

The Skew-T/Hodograph Analysis and Research Program (SHARP; Hart and Korotky 1991) computed a CAPE of 1864 J kg^{-1} for a surface-based parcel. Craven et al. (2002) determined that an actual parcel associated with convective development is better represented by a parcel whose temperature and moisture are given by an average over the lowest 100 hPa rather than a surface-based parcel. With use of such a parcel the CAPE was 791 J kg^{-1}, less than that for a surface-based parcel but still indicative of an unstable atmosphere.

Convergence along a cloud line, presumably composed of a string of three outflow boundaries from the previous night's convection, provided the lifting mechanism to initiate the thunderstorms. Geostationary Operational Environmental Satellite-West (GOES-West) visible imagery from 1715 UTC shows a continuous cloud line, composed of three arc-shaped cloud sections in eastern New Mexico and western Texas (Fig. 3a). Their appearance, particularly the two southernmost sections, is similar to cloud features associated with thunderstorm outflow boundaries. Purdom (1973) first showed that the leading edge of a thunderstorm's cold pool often contains an arc-shaped line of convective clouds, which he named arc clouds.

The ability of thunderstorm outflow boundaries to initiate convection has been noted in the literature. In particular, the intersection of an arc cloud with another
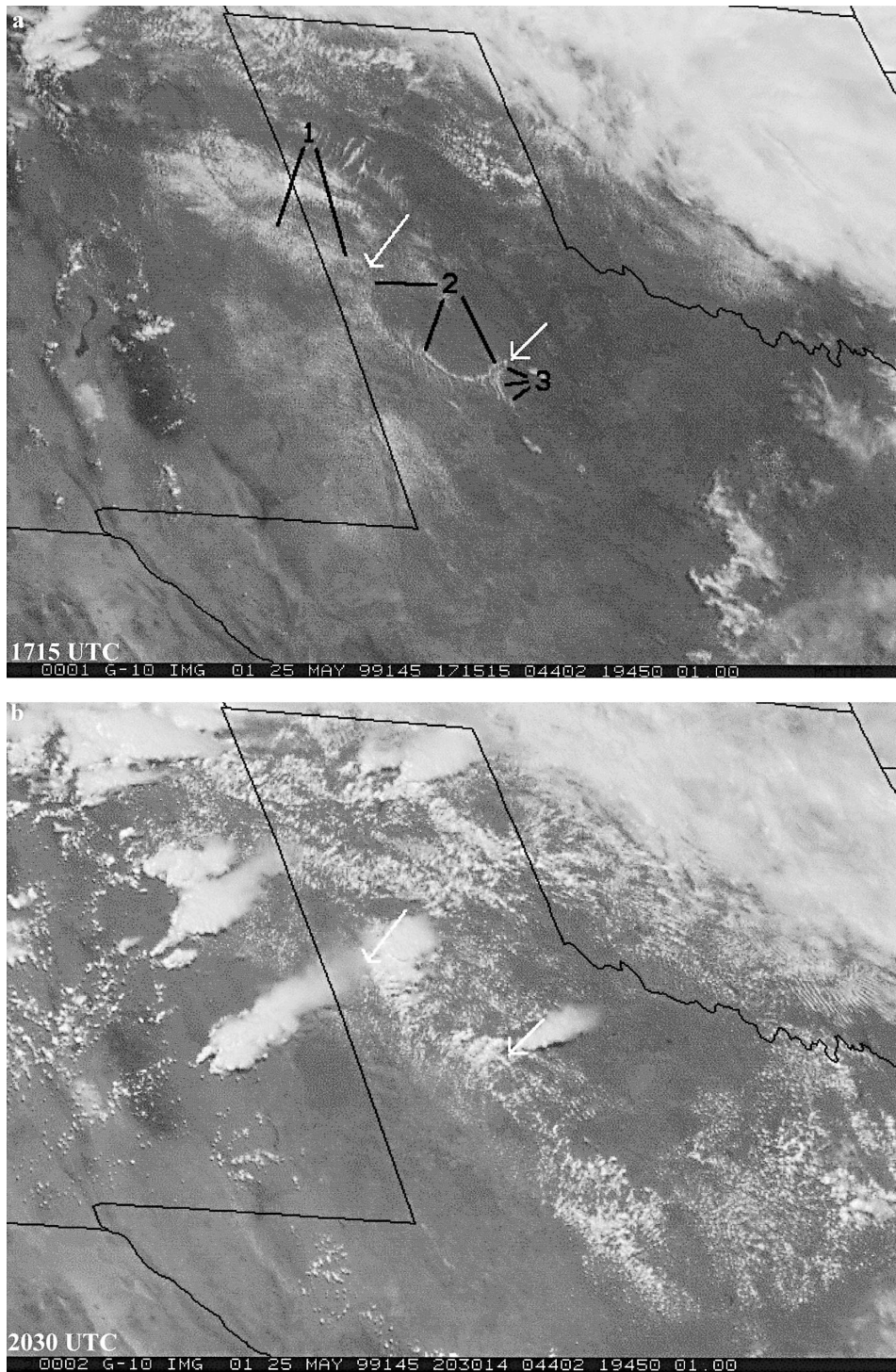
FIG. 3. GOES-West visible imagery showing the development of convection on 25 May 1999. Black lines labeled 1, 2, and 3 point to the three individual sections that make up the cloud line along which thunderstorms developed. The white arrows point to the two cusps that formed between the three sections of the line and correspond to the strongest convection that developed along the line.
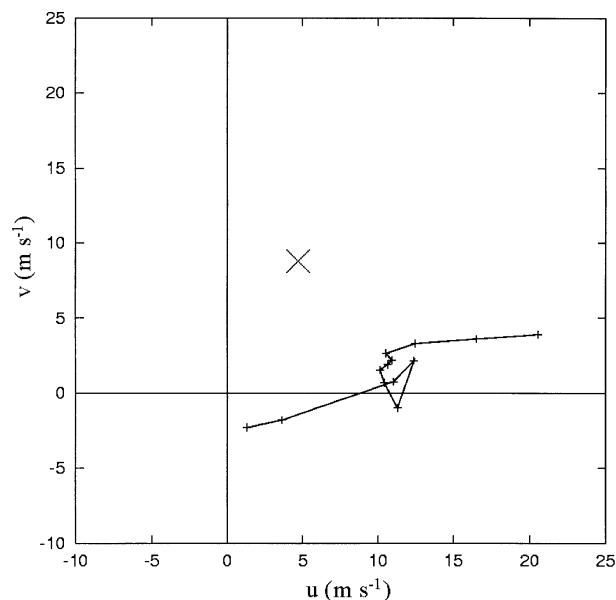
FIG. 4. The 0–6-km hodograph from the 1800 UTC sounding at Amarillo for 25 May 1999. Tick marks are every 500 m AGL, statrting at the surface. The storm motion vector of the left mover is marked with ×.

arc cloud or with another surface boundary, such as a cold front, has been shown to be a favorable location for convective initiation (Purdom 1976; Weaver and Nelson 1982; Scofield and Purdom 1986). In the 1715 UTC image, two distinct cusps exist where the individual sections that make up the line intersect. These cusps have been marked with white arrows in the figure and were evidently associated with enhanced convergence along the line, because the strongest convection developed in the vicinity of these features (Fig. 3b). The storm that formed on the northwestern cusp is the subject of this note.

c. Vertical wind shear

The combination of moisture, instability, and a lifting mechanism suggests the probability of deep convection, but not the form that the convection is likely to assume, namely, the presence or absence of updraft rotation, often referred to as supercellular and multicellular convection, respectively. The tendency for an updraft to develop rotation has been attributed to the vertical wind shear in the storm's environment (Klemp 1987). The vertical wind profile from the 1800 UTC Amarillo sounding is shown in the 0–6-km hodograph (Fig. 4). Also depicted in the hodograph is the storm motion of the left mover, which was measured by radar data to be 10 m s^{-1} from 208°. Three parameters that measure the potential of the atmosphere to produce thunderstorms with rotating updrafts are the 0–6-km wind shear (vector difference), the bulk Richardson number, and the storm-relative helicity.

Bunkers (2002) found that 95% of both left- and right-moving supercells form in an environment with a 0–6-km shear magnitude greater than 13 m s^{-1}. At 1800 UTC the 0–6-km shear over Amarillo was 20 m s^{-1}. Not only do most supercells form in a sheared environment, but thunderstorms without rotating updrafts are less likely to form in a sheared environment. Rasmussen and Blanchard (1998) report that only 25% of nonsupercell thunderstorms form in an environment containing a shear from the boundary layer to 6 km of 16 m s^{-1} or greater.[1] Because the thunderstorms formed between Amarillo and Lubbock, the wind shear from the surface to 6 km and from the boundary layer to 6 km from the 2046 UTC velocity azimuth display wind profile from the Weather Surveillance Radar-1988 Doppler (WSR-88D) located at Lubbock were also computed. Both values were 23 m s^{-1}. Hence, the 0–6-km shear on 25 May 1999 was indicative of an environment favorable to the development of thunderstorms with rotating updrafts.

The bulk Richardson number (Weisman and Klemp 1982, 1984) is given by $R = \text{CAPE}/\frac{1}{2}(\overline{u}^2 + \overline{v}^2)$, where CAPE is measured using a surface-based parcel, and $\overline{u}$ and $\overline{v}$ are the two components of the difference between the 0–6-km density-weighted mean wind and the 0–500-m mean wind. Weisman and Klemp (1984) show that rotating updrafts are favored when R lies between 15 and 45 and that multicellular convection is favored for values of R of greater than 45. SHARP software was used to calculate the bulk Richardson number for the 1800 UTC Amarillo sounding. With the surface-based CAPE value of 1864 J kg^{-1}, $R = 53$. In contrast to the 0–6-km shear value, the bulk Richardson number suggested an environment favorable to multicellular convection.

A third measure of vertical wind shear, the storm-relative helicity, was also assessed. Rasmussen and Blanchard (1998) investigated storm-relative helicity, among other parameters, in terms of its ability to differentiate among storm types. They found that supercell thunderstorms with hail greater than 5.07 cm but without tornadoes or with weak (F0 or F1 on the Fujita scale) tornadoes generally have storm-relative helicities between 64 and 208 m^2 s^{-2}. Although they investigated right-moving thunderstorms, it is assumed that these magnitudes are applicable to left movers. For left movers, the sign will be reversed, however, so that, for the above category of thunderstorm, storm-relative helicities of −64 to −208 m^2 s^{-2} would be expected. With the SHARP software package, a storm-relative helicity of −93 m^2 s^{-2} was computed from the 1800 UTC sound-

---

[1] Bunkers (2002) and Rasmussen and Blanchard (1998) compute wind shear slightly differently. The former uses the difference between the 6-km and surface winds, whereas the latter uses the difference between the 6-km and the 0–500-m (boundary layer) mean wind. The Amarillo sounding has a surface-to-6-km shear of 20 m s^{-1} and a shear from the boundary layer to 6 km of 19 m s^{-1}.
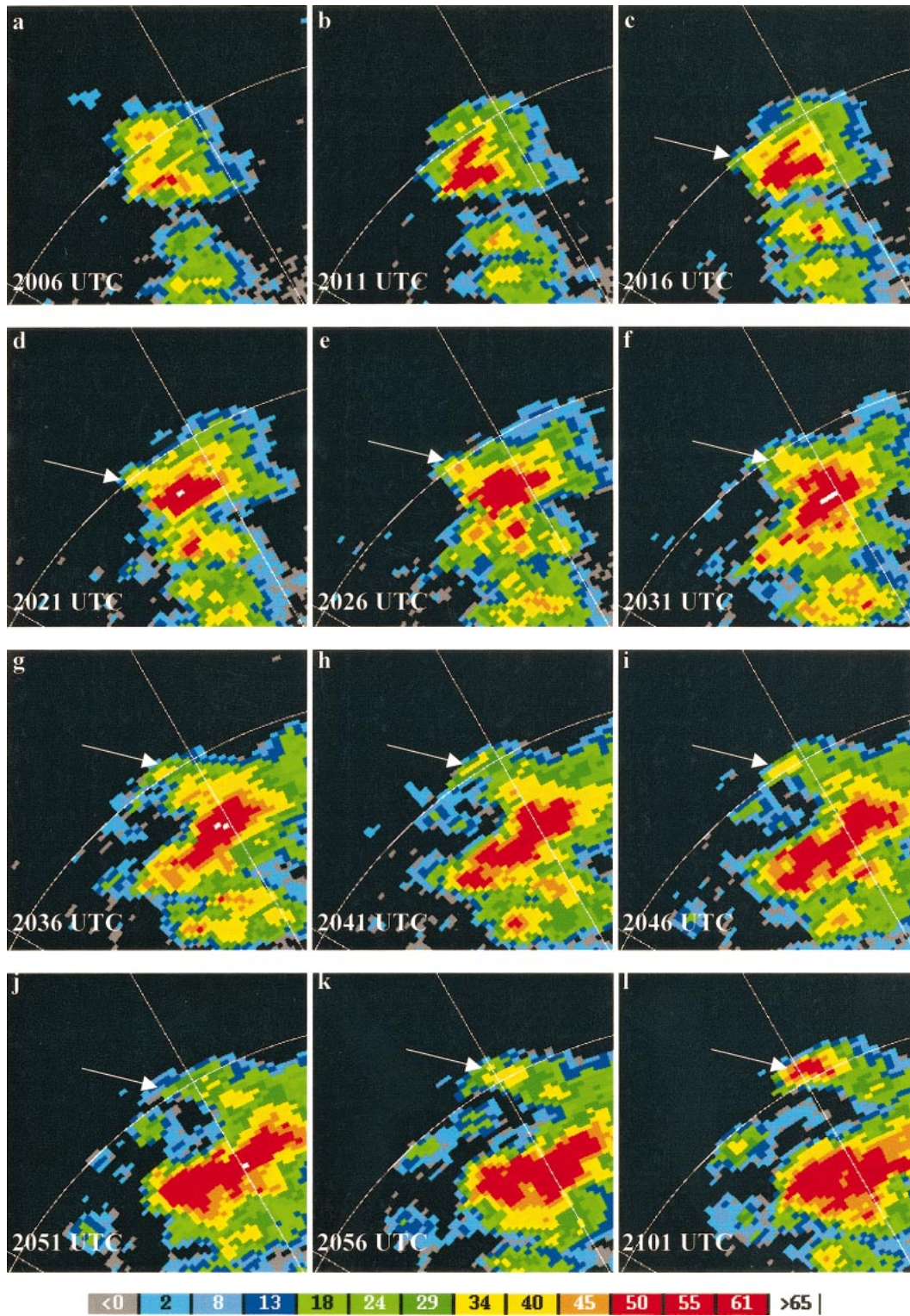
FIG. 5. Radar reflectivity on 25 May 1999 from the WSR-88D located at Lubbock. Tilt angle is 0.5°. White arrows point to the left mover. Range ring in panels is at 100 km.
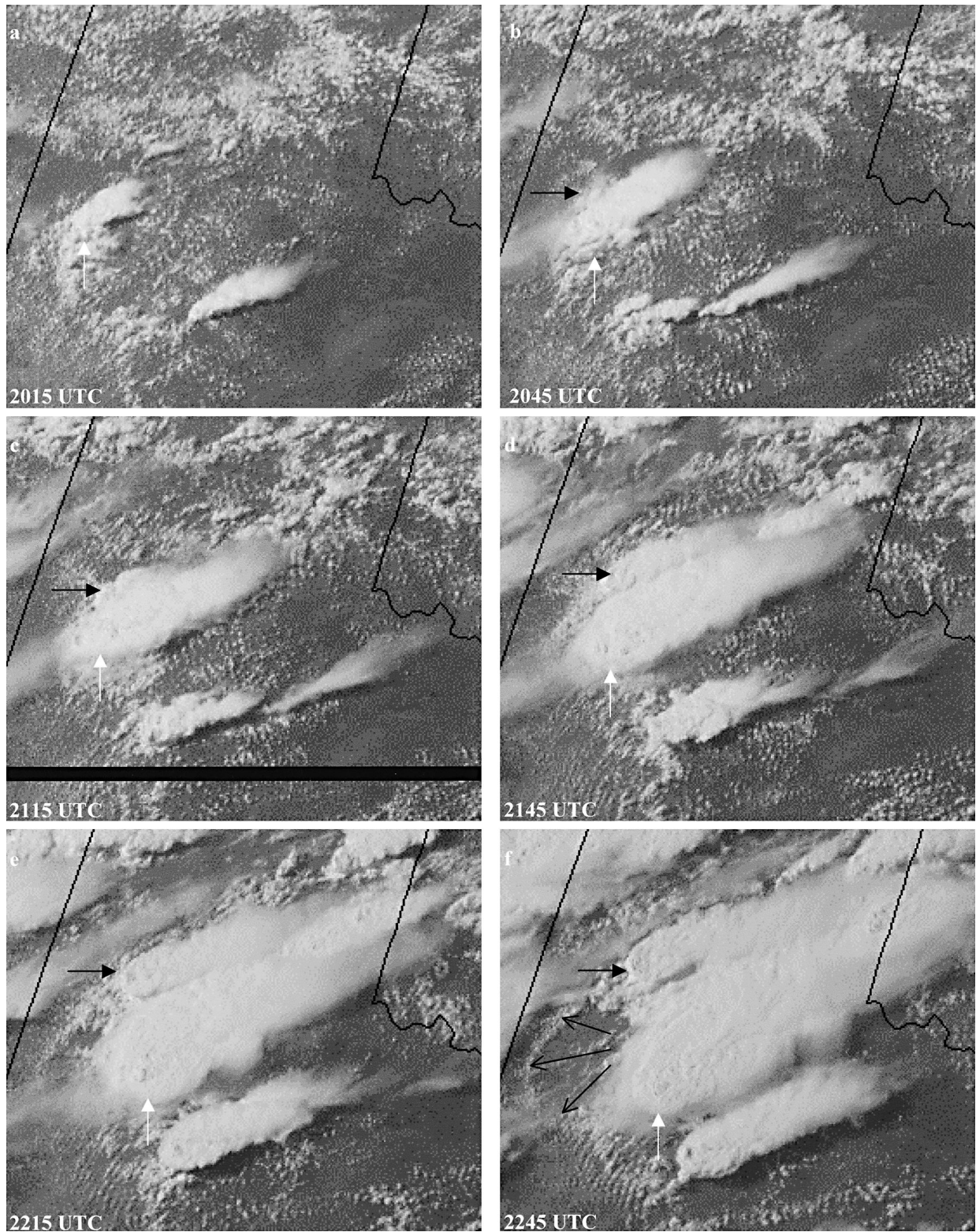
FIG. 6. GOES-East visible imagery showing the left- and right-moving thunderstorms of 25 May 1999. White arrows point to the right-moving thunderstorm, black arrows with enclosed tips to the left-moving thunderstorm, and black arrows without enclosed tips in (f) point to the arc cloud.
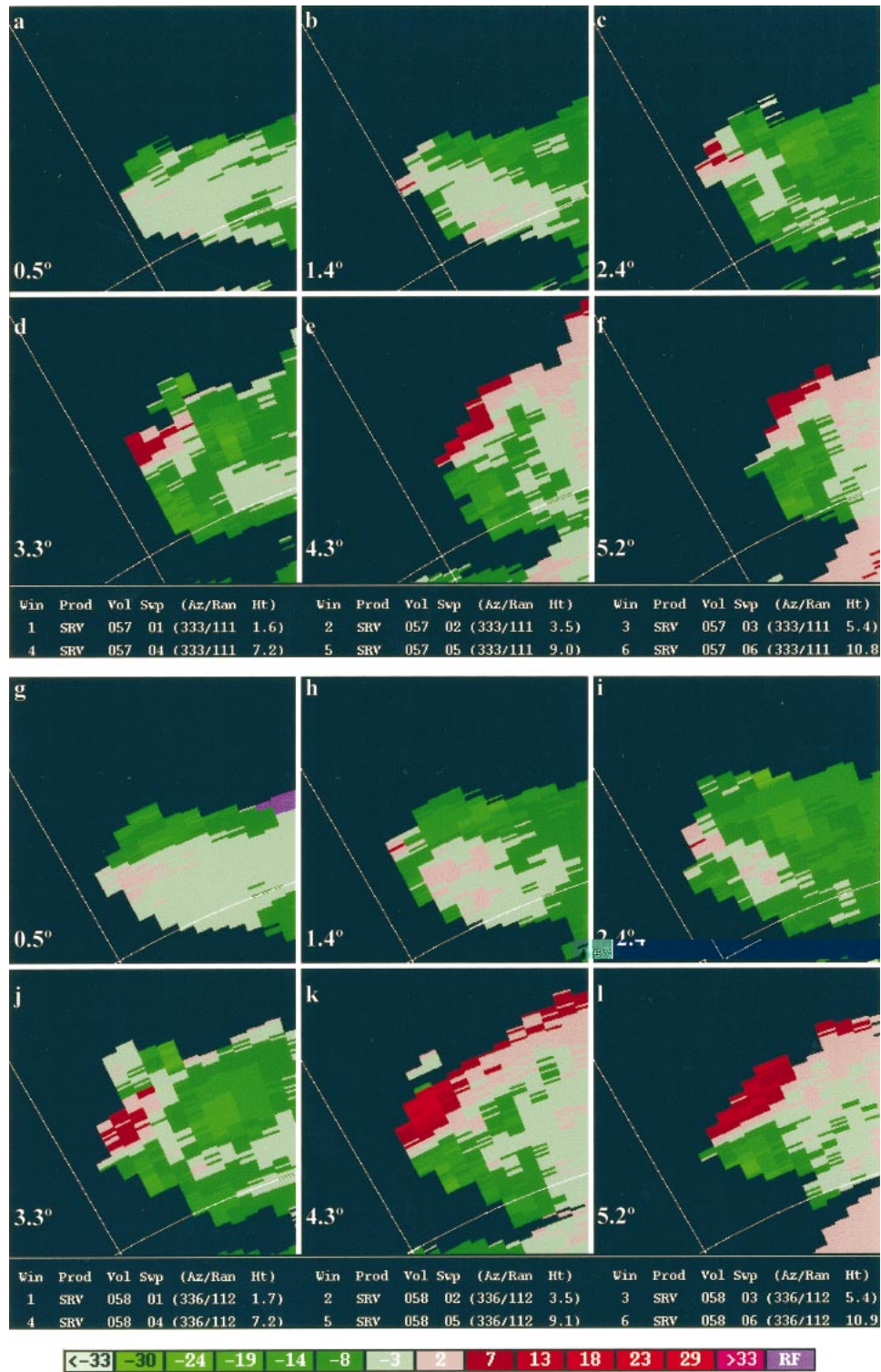
FIG. 7. First six elevation sweeps of storm-relative radial velocity from the Lubbock WSR-88D of the left-moving thunderstorm of 25 May 1999. (a)–(f) From 2116 UTC; (g)–(l) from 2121 UTC.
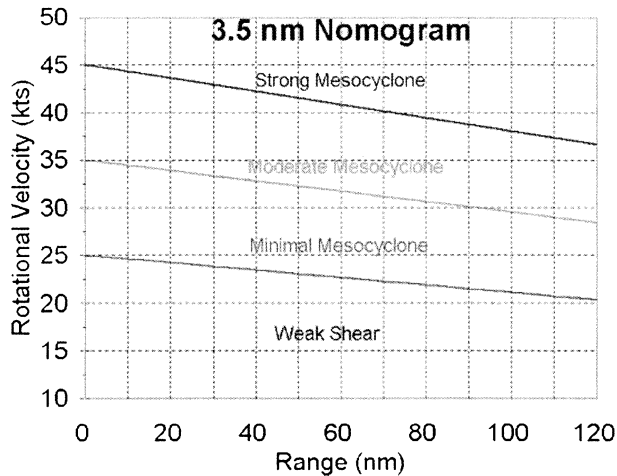
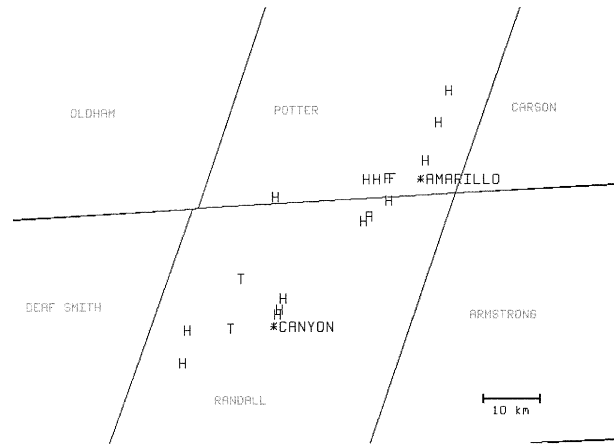FIG. 8. Nomogram for mesocyclones of 3.5 n mi (6.5 km) in diameter.

FIG. 9. Severe weather reports associated with the left mover from 2244 UTC 25 May to 0005 UTC 26 May 1999 (T, tornado; H, hail > 1.9 cm; F, flash flood). Canyon and Amarillo are noted with an asterisk, and the counties are labeled.

ing at Amarillo, a value commensurate with the severity of the storm when the above results of Rasmussen and Blanchard (1998) are considered.

3. Characteristics of the left mover

a. Formation

Using radar data, Achtemeier (1969) and Burgess et al. (1976) describe the splitting of a thunderstorm as a mitosis-like process, in which the left-moving and right-moving members form from a single storm. Numerical simulations (Klemp and Wilhelmson 1978; Wilhelmson and Klemp 1978; Rotunno and Klemp 1982) have also shown this behavior. A sequence of WSR-88D reflectivity images from Lubbock shows the development of the left mover of 25 May 1999 (Fig. 5). By 2011 UTC, the thunderstorm that formed along the northwestern cusp of the convergence line discussed in the previous section was producing 61-dBZ reflectivity returns 90 km northwest of Lubbock. At 2016 UTC, reflectivities in the 30–40-dBZ range extended to the northwest of the core. This extension proceeded to pull away from the storm until a complete separation of the 34-dBZ contour appeared at 2036 UTC. This storm continued to move away from the initial storm but underwent a weakening at 2051 UTC. Over the next 10 min, however, the storm rapidly reintensified to the 50-dBZ range, an intensity equal to that of the initial storm, which at this point could be considered as the right mover. Still, the left mover was considerably smaller than the right mover in areal extent. This size discrepancy remained throughout the left mover's lifetime.

GOES-East visible imagery also shows the development of the left mover (Fig. 6). The left mover is first seen at 2045 UTC as a cloud mass on the northwest side of the original storm. With time, the left mover continued to develop and to propagate away from the right mover as in the radar imagery. The sequence re-veals that the left mover propagated northward with the northward-moving outflow boundary associated with the initial storm. The reintensification of the left mover seen in the radar images after 2051 UTC may have been due, in part, to convergence along this outflow boundary.

b. Storm rotation

WSR-88D storm-relative radial velocity data were used to investigate the rotational characteristics of the left mover. The first six elevation sweeps for the 2116 UTC scan from the Lubbock WSR-88D indicate Doppler signatures typical of a rotating thunderstorm (Figs. 7a–f). The 0.5° tilt shows the convergence at low levels of the thunderstorm, with inbound velocities increasing with distance from the radar. The 1.4°, 2.4°, and 3.3° tilts indicate the mesoanticyclone, with outbound velocities (red) to the left of inbound velocities (green). Given the elevation angles and the 111-km distance from the radar, the mesoanticyclone was located between 3.5 and 7.2 km, a depth of 3.7 km. The 4.3° and 5.2° tilts show the storm-top divergence in the 9–11-km layer, with outbound velocities increasing with distance from the radar. The equilibrium level for a surface-based parcel lifted along Amarillo's 1800 UTC sounding was computed by SHARP to be at 10 607 m, located within the divergence layer.

Andra (1997) discusses a nomogram used to measure the strength of a rotating thunderstorm (Fig. 8). The nomogram was developed for mesocyclones but will be assumed to be valid for application to mesoanticyclones. The abscissa of the nomogram contains the range of the storm, in this case 111 km (60 n mi). The ordinate contains the rotational velocity v_r, where $v_r = (|v_{inbound}| + |v_{outbound}|)/2$. The rotational velocity was measured using the 2.4° tilt, which is the middle sweep of the
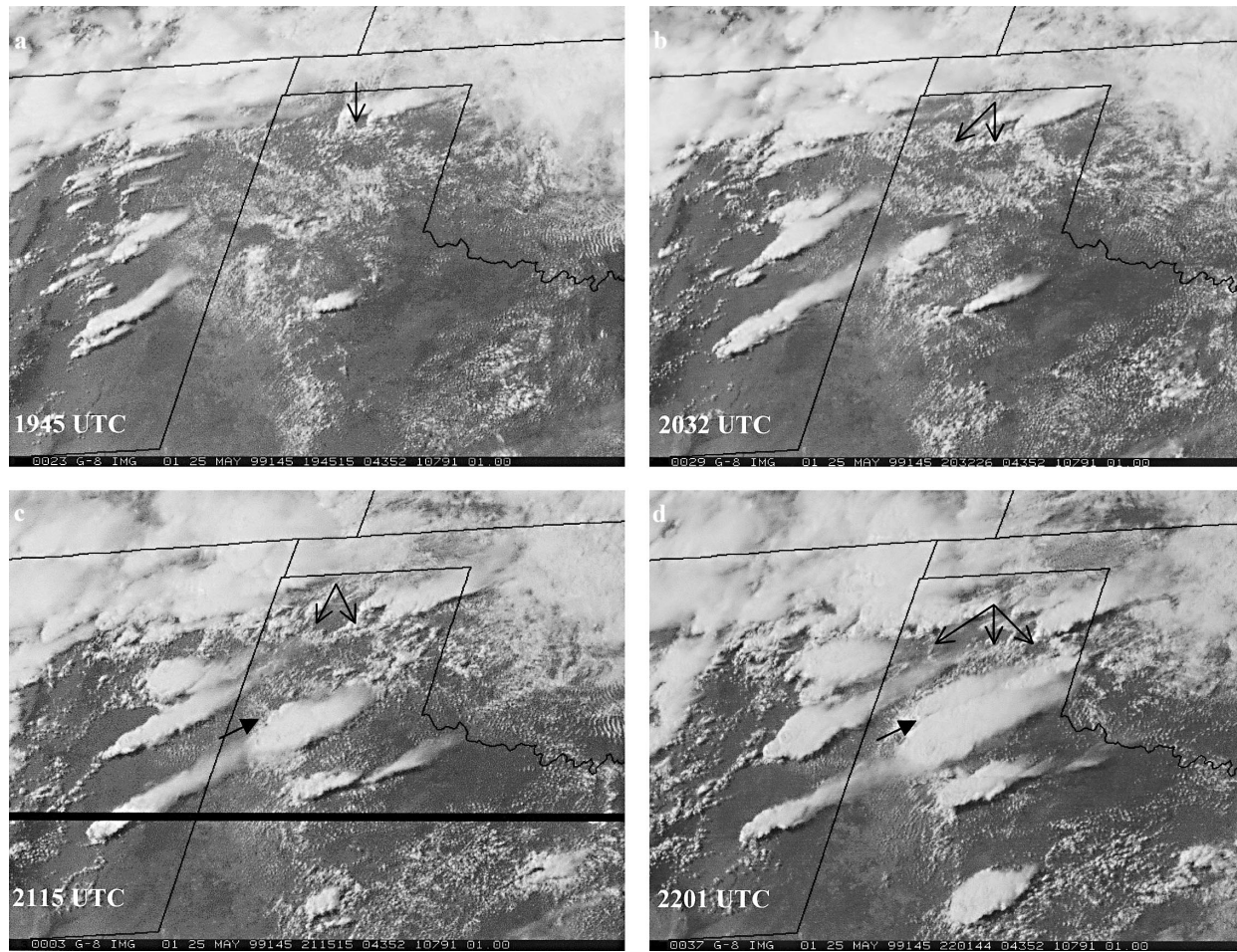
FIG. 10. GOES-East visible imagery showing the approach of the left-moving thunderstorm and a boundary moving southward from the northern portion of the Texas Panhandle. Black arrows with enclosed tips denote the left-moving thunderstorm, and black arrows without enclosed tips denote the southward-moving boundary.

mesoanticyclone. The maximum inbound velocity was -33 m s^{-1}, and the maximum outbound velocity was 7 m s^{-1}, giving a rotational velocity of 20 m s^{-1} (39 kt). The mesoanticyclone diameter, as measured between these velocity maxima, was 7.4 km (4 n mi). The diameter of the mesoanticyclone is thus close to the 3.5 n mi for which the nomogram was developed. Using a distance of 111 km (60 n mi) and a rotational velocity of 20 m s^{-1} (39 kt), the nomogram indicates the left mover to be a moderate mesoanticyclone.

To demonstrate the time continuity of the mesoanticyclone, the first six elevation sweeps of the next volume scan are also given in Figs. 7g–l. As with the 2116 UTC scans, the 2121 UTC scans show convergence at low levels, anticyclonic rotation at the middle three sweeps, and divergence at the upper levels. Again using the 2.4° data, the maximum outbound velocity was 7 m s^{-1} and the maximum inbound velocity was -30 m s^{-1}, resulting in a rotational velocity of 18.5 m s^{-1} (36 kt). The width of the mesoanticyclone was measured as 9.3 km (5 n mi). The distance between the radar and the

storm was again 111 km (60 n mi). The nomogram thus continued to indicate a moderate mesoanticyclone. Rotation appeared to persist after 2121 UTC but became difficult to quantify as range folding became an issue.

c. Storm severity

From its inception around 2036 UTC 25 May 1999 until 0015 UTC 26 May 1999, after which it merged with another storm, the left mover was responsible for 15 reports of hail diameters of greater than 1.9 cm (including reports of up to 7 cm), 3 flash-flood reports, and 2 tornado reports (NCDC 1999). In relation to the hail reports, numerous flare echoes, or three-body-scatter spikes (Wilson and Reum 1988), were identified with this storm. The first tornado report was from 5 mi west of Canyon, Texas, at 2258 UTC (Fig. 9). The report came from the Canyon Fire Department, which is considered to be a reliable source by the National Weather Service Forecast Office in Lubbock. The reliability of the source is important for an F0 or F1 tornado, because
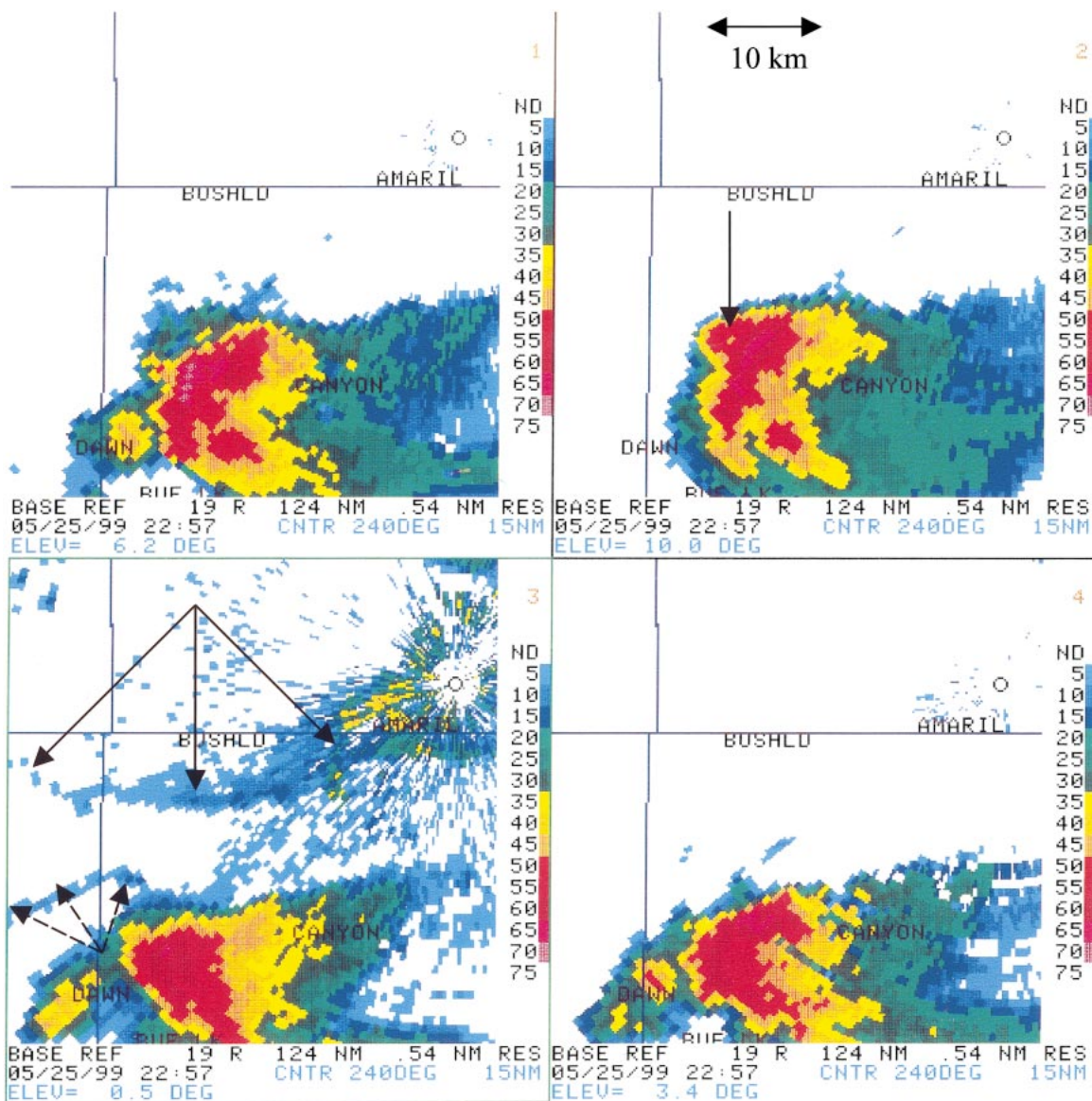
FIG. 11. The 2257 UTC reflectivity data from the WSR-88D located at Amarillo. The elevation angle of the scan is listed underneath each image. In the 0.5° tilt, the southward-moving boundary is denoted by solid arrows and the left mover's own outflow boundary is denoted by dashed arrows. In the 10.0° tilt, the arrow points to a possible bounded weak echo region.

reports of weak tornadoes can be unreliable (Markowski et al. 1998). The report mentions a path 75 ft wide, extending 1/3 mi. The second tornado report was from members of the public, who reported a tornado 8 mi northwest of Canyon between 2305 and 2308 UTC. The pathwidth was 75 ft, and the pathlength was estimated at 1 mi. The tornado caused $10,000 of damage to an outbuilding. The sense of rotation of the tornadoes is not known.

Although rated F0, the tornadoes are of interest because, to the authors' knowledge, only four other tornadic left movers have been cited in the meteorological literature. Brown and Meitín (1994) cite three examples

from Oklahoma, and Monteverdi et al. (2001) discuss a tornadic left-moving thunderstorm in California.

The tornadic development of 25 May 1999 may have been due to the interaction of the left mover with a boundary moving southward from the northern Texas Panhandle. Markowski et al. (1998) note that during the Verifications of the Origins of Rotation in Tornadoes Experiment, nearly 70% of significant tornadoes were associated with preexisting boundaries not associated with the thunderstorm itself, a front or outflow boundary from another thunderstorm, for example. Thunderstorms that do produce tornadoes in conjunction with a preexisting boundary generally do so from 10 km in front

of the boundary (warm side) to 30 km behind the boundary (cold side). Such boundaries provide vertical and horizontal vorticity that may be tilted and/or stretched to aid in tornadogenesis.

Visible satellite imagery (Fig. 10) shows the approach of the thunderstorm and the boundary, which may be associated not only with the outflow from the thunderstorm in the northeast Texas Panhandle, but also with a larger-scale advance of cooler air southward into the Texas Panhandle. After the 2201 UTC image, clouds largely obscured the view of the boundary from the satellite, but the approach of the left mover and the boundary could still be tracked by the WSR-88D located in Amarillo. At 2257 UTC, just before the first tornado report, the storm was about 10 km on the warm side of the southward-moving boundary (Fig. 11), consistent with the results of Markowski et al. (1998). The reflectivity patterns of the four elevation angles indicate a weak echo region, with a possible bounded weak echo region (Weisman and Klemp 1986) indicated in the $10.0°$ scan as a small area of 45-dBZ returns enclosed in a region of returns of greater than 50 dBZ. Also evident is the left mover's own low-level outflow. Storm rotation during this period was not evident in the velocity data available.[2]

4. Summary

The atmosphere over the Texas Panhandle on 25 May 1999 contained the necessary ingredients for the development of severe weather, namely, moisture, instability, and a lifting mechanism. The lifting mechanism was seen in satellite imagery as a single cloud line composed of three individual arc-shaped sections, likely the result of overnight convection. At the two cusps that defined the intersection of the individual components of the line, convergence was evidently enhanced, because strong convection occurred in these locations. The thunderstorm that formed along the northwestern cusp produced a left mover that traveled northward along the initial thunderstorm's low-level outflow boundary. This long-lived left mover contained a mesoanticyclone and was responsible for numerous severe weather reports.

Of particular interest were the reports of two tornadoes near Canyon. It is possible that the tornadoes occurred in conjunction with the interaction of the left mover with a southward-moving boundary, following the process outlined in Rasmussen and Blanchard (1998). To the authors' knowledge, this storm is only the fifth tornadic left-moving thunderstorm to be documented in the meteorological literature.

REFERENCES

Achtemeier, G. L., 1969: Some observations of splitting thunderstorms over Iowa on August 25–26, 1965. Preprints, *Sixth Conf. on Severe Local Storms,* Chicago, IL, Amer. Meteor. Soc., 89–94.

Andra, D. L., Jr., 1997: The origin and evolution of the WSR-88D mesocyclone recognition nomogram. Preprints, *28th Conf. on Radar Meteorology,* Austin, TX, Amer. Meteor. Soc., 364–365.

Brown, R. A., and R. J. Meitín, 1994: Evolution and morphology of two splitting thunderstorms with dominant left-moving members. *Mon. Wea. Rev.,* **122,** 2052–2067.

Bunkers, M. J., 2002: Vertical wind shear associated with left-moving supercells. *Wea. Forecasting,* **17,** 845–855.

Burgess, D. W., L. R. Lemon, and G. L. Achtemeier, 1976: Severe storm splitting and left-moving storm structure. *The Union City, Oklahoma Tornado of 24 May 1973,* R. A. Brown, Ed., NOAA Tech. Memo. ERL NSSL-80, National Severe Storms Laboratory, 63–66.

Craven, J. P., R. E. Jewell, and H. E. Brooks, 2002: Comparison between observed convective cloud-base heights and lifting condensation level for two different lifted parcels. *Wea. Forecasting,* **17,** 885–890.

Davies-Jones, R. P., 1985: Tornado dynamics. *Thunderstorm Morphology and Dynamics,* 2d ed., E. Kessler, Ed., University of Oklahoma Press, 197–236.

Grasso, L. D., and E. R. Hilgendorf, 2001: Observations of a severe left-moving thunderstorm. *Wea. Forecasting,* **16,** 500–511.

Hammond, G. R., 1967: Study of a left moving thunderstorm of 23 April 1964. ESSA Tech. Memo. IERTM-NSSL-31, Norman, OK, 75 pp.

Hart, J. A., and W. D. Korotky, 1991: The SHARP workstation—v1.50. A skew *T*/hodograph analysis and research program for the IBM and compatible PC. User's manual, NOAA/NWS Forecast Office, Charleston, WV, 62 pp.

Johns, R. H., and C. A. Doswell III, 1992: Severe local storms forecasting. *Wea. Forecasting,* **7,** 588–612.

Klemp, J. B., 1987: Dynamics of tornadic thunderstorms. *Annu. Rev. Fluid Mech.,* **19,** 369–402.

——, and R. B. Wilhelmson, 1978: Simulations of right and left moving storms produced through storm splitting. *J. Atmos. Sci.,* **35,** 1097–1110.

Markowski, P. M., E. N. Rasmussen, and J. M. Straka, 1998: The occurrence of tornadoes in supercells interacting with boundaries during VORTEX-95. *Wea. Forecasting,* **13,** 852–859.

Monteverdi, J. P., W. Blier, G. Stumpf, W. Pi, and K. Anderson, 2001: First WSR-88D documentation of an anticyclonic supercell with anticyclonic tornadoes: The Sunnyvale–Los Altos, California, tornadoes of 4 May 1998. *Mon. Wea. Rev.,* **129,** 2805–2814.

NCDC, 1999: *Storm Data.* Vol. 41, No. 5, 372 pp.

Nielsen-Gammon, J. W., and W. L. Read, 1995: Detection and interpretation of left-moving severe thunderstorms using the WSR-88D: A case study. *Wea. Forecasting,* **10,** 127–140.

Purdom, J. F. W., 1973: Meso-highs and satellite imagery. *Mon. Wea. Rev.,* **101,** 180–181.

——, 1976: Some uses of high-resolution GOES imagery in the mesoscale forecasting of convection and its behavior. *Mon. Wea. Rev.,* **104,** 1474–1483.

Rasmussen, E. N., and D. O. Blanchard, 1998: A baseline climatology of sounding-derived supercell and tornado forecast parameters. *Wea. Forecasting,* **13,** 1148–1164.

Rotunno, R., and J. B. Klemp, 1982: The influence of the shear-induced pressure gradient on thunderstorm motion. *Mon. Wea. Rev.,* **110,** 136–151.

Scofield, R. A., and J. F. W. Purdom, 1986: The use of satellite data

---

[2] Level-IV data were used in lieu of level-II data, which are not available from Amarillo for this case.

for mesoscale analyses and forecasting applications. *Mesoscale Meteorology and Forecasting,* P. S. Ray, Ed., Amer. Meteor. Soc., 118–150.

Weaver, J. F., and S. P. Nelson, 1982: Multiscale aspects of thunderstorm gust fronts and their effects on subsequent storm development. *Mon. Wea. Rev.,* **110,** 707–718.

Weisman, M. L., and J. B. Klemp, 1982: The dependence of numerically simulated convective storms on vertical wind shear and buoyancy. *Mon. Wea. Rev.,* **110,** 504–520.

——, and ——, 1984: The structure and classification of numerically simulated convective storms in directionally varying wind shears. *Mon. Wea. Rev.,* **112,** 2479–2498.

——, and ——, 1986: The characteristics of isolated convective storms. *Mesoscale Meteorology and Forecasting,* P. S. Ray, Ed., Amer. Meteor. Soc., 331–358.

Wilhelmson, R. B., and J. B. Klemp, 1978: A numerical study of storm splitting that leads to long-lived storms. *J. Atmos. Sci.,* **35,** 1974–1986.

Wilson, J. W., and D. Reum, 1988: The flare echo: Reflectivity and velocity signature. *J. Atmos. Oceanic Technol.,* **5,** 197–205.